Journal of Applied Fluid Mechanics, Vol. 11, No. 4, pp. 885-894, 2018.
Available online at www.jafmonline.net, ISSN 1735-3572, EISSN 1735-3645.
DOI: 10.29252/jafm.11.04.28214

CFD Investigation on the Steady Interaction between an Offset Jet and an Oblique Wall Jet

N. Hnaien[1], S. Marzouk[1], L. Kolsi[2,1,†], A. A. A. A. Al-Rashed[3], H. Ben Aissia[1] and J. Jay[4]

[1.] *Unit of Metrology And Energy Systems, National Engineering School of Monastir, University of Monastir, Tunisia*
[2.] *College of Engineering, Mechanical Engineering Department, Haïl University, Saudi Arabia*
[3.] *Department. of Automotive and Marine Engineering Technology, College of Technological Studies, The Public Authority for Applied Education and Training, Kuwait*
[4.] *Thermal Center of Lyon (CETHIL - UMR CNRS 5008), INSA Lyon, France*

†*Corresponding Author Email: lioua_enim@yahoo.fr*

(Received July 17, 2017; accepted February 19, 2018)

ABSTRACT

In this paper a CFD investigation on the interaction between an offset jet and an oblique wall jet using two-dimensional steady RANS equations is performed. This combination is denoted WOJ (Wall Offset jets). Several turbulence models such as the standard k-ω, SST k-ω, standard k-ε, RNG k-ε and realizable k-ε models are tested in the present study. A parametric study is performed to highlight the wall inclination effect on the WOJ flow maximum velocity decay as well as the shear layers spreading. Comparison between combined wall and offset jet (WOJ) and single offset jet (SOJ) flows is also established. Results show that increasing the wall inclination improves the combined wall and offset jets flow spreading. Furthermore, the outer shear layers spreading, is better than the inner shear layers one. Comparing to the combined wall and offset jet flow (WOJ), a better spreading is found in the case of single offset jet flow (SOJ).

Keywords: Combined jets; Inclination; Maximum velocity; Shear layer; Steady RANS; Turbulent flow

NOMENCLATURE

a	grid spacing
d	nozzle width
e	grid expansion ratio
h	offset ratio
H	dimensionless offset ratio H=h/d
I	turbulence intensity
k	turbulent kinetic energy
l	nozzle length
p	static pressure
P	dimensionless pressure $P = \frac{p - p_{amb}}{\rho u_0^2}$
u	longitudinal velocity
U	dimensionless longitudinal velocity U=u/u_0
v	transverse velocity
V	dimensionless transverse velocity V=v/u_0
ω	turbulent kinetic energy dissipation rate
x	longitudinal coordinate
X	dimensionless longitudinal coordinate X=x/d
y	transverse coordinate
Y	dimensionless transverse coordinate Y=y/d
y(0.5)	dynamic half width: transverse distance between U_m and 0.5×U_m
Y(0.5)	dimensionless dynamic half-with Y(0.5)=y(0.5)/d

Subscripts

amb	ambient value
0	outlet value (at nozzles exit)
1	outer shear layers
2	inner shear layers
t	turbulent value
'	opposite segments

Greek symbols

υ	kinematic viscosity
ρ	fluid density

Abbreviations

CP	Combined Point
ISL	Inner Shear Layers
LWJ	Lower Wall Jet
MP	Merge Point
OSL	Outer Shear Layers
SOJ	Single Offset Jet Flow
UOJ	Upper Offset Jet
WOJ	Combined Wall And Offset Jet Flow
2D	Two-Dimensional

1. INTRODUCTION

The flows in the wall vicinity are frequently encountered in several industrial applications such as air-conditioning, heat exchanger and waste water evacuation process. When air jet is discharged from a nozzle situated in the wall vicinity, a depression region appears along the zone between the jet and the wall due to the air entrainment through the flow shears layers. Consequently a flow deviation toward the wall occurs. This phenomenon is called "Coanda effect" and the flow is named single offset jet (SOJ). When a second wall jet is placed parallel to the offset jet, a multi-jets flow which combine a wall jet and an offset jet is obtained, this combination is denoted WOJ (wall offset jet). When the second wall jet is inclined with respect to the horizontal direction, this combination is called oblique WOJ flow. This kind of flow is specially applied in air-conditioning materials such as adjustable air diffuser with inclined flaps.

Wang and Tan (2007) were ones of the first who have worked on combined wall and offset jet flow (WOJ). Using PIV (Particle Image Velocimetry), they experimentally studied the WOJ characteristics for a Reynolds number and an offset ratio respectively equal to Re=10000 and H=2. Using water as working fluid, the flow characteristics such as time average velocity, shear stress and flow spreading in term of dynamic half-width at different shear layers are identified. During their experimental investigation, Wang and Tan (2007) noted, along the inner shear layers of the WOJ flow, the existence of periodical large scale Karman-like vortices. The existence of these vortices causes a periodic mutual interaction between the wall and offset jets.

Vishnuvardhanarao and Kumar (2009) performed a numerically investigation on the thermal characteristics of combined wall and offset jets flow WOJ with the help of standard k-ε turbulence model. The flow is assumed to be incompressible and in a steady state. Simulation was performed for various Reynolds numbers between Re=10000 and Re=40000 and for constant Prandtl number (Pr=0.7). Twin boundary conditions are adopted at the horizontal wall such as constant heat flux and constant temperature. Vishnuvardhanarao and Kumar (2009) found that downward of the nozzles plate, the local Nusselt number Nu increases when increasing either the wall jet or the offset jet exit velocity. They also found more intense heat transfer exchanged between the whole flow and the wall for constant heat flux boundary condition.

Numerical study on turbulent characteristics of combined wall and offset jets flow (WOJ) was carry out by Kumar and Das (2011) using standard k-ε turbulence model with high Reynolds number. The adopted nozzle spacing, Reynolds number, turbulence intensity and Prandtl number were respectively 9, 20000, 5% and 0.7. Their code validation was realized on the experimental results of Pelfrey and Liburdy (1986) and numerical ones of Vishnuvardhanarao and Das (2008) for single offset jet case (SOJ). Kumar and Das (2011) noted negative static pressure along the initial flow zone (called the converging zone or the recirculation zone) as well as along the outer shear layers. Different locations of the flow characteristics points such as the merge point, the combining point and the recirculation vortices centers are identified. The obtained numerical results indicate that, along the initial flow zone (the converging zone) and the latter flow zone (the combined zones) the maximum longitudinal velocity of combined wall and offset jet flow (WOJ) decays in a similar way to that of a single offset jet. On the other hand, Kumar and Das (2011) noted that the jet spreading in term of dynamic half-width similar to that of a single offset jet (SOJ) for longitudinal locations flow below X=7.5. It has been also found that at X=10, the jet half-width reaches its maximum value.

The nozzles spacing effect on turbulent 2D WOJ flow along the converging zone was numerically investigated by Mondal *et al*. (2014) using the RANS (Reynolds Averaged Navier-Stokes equations) method. Calculations were performed for different nozzle spacing and various nozzles widths. During this study, the authors noted the presence of Karman vortex along the initial flow zone (the converging zone) for non-dimensional nozzle spacing between 0.7 and 2.1. However, for nozzles spacing outside this range, twin steady counter rotating vortices are formed along this flow zone.

Kumar (2015) was numerically simulated combined wall and offset jets flow for a Reynolds number Re=15000, an offset ratio H=7, a nozzle width d=12.5 mm and a nozzle exit velocity u_0 = 17.4m/s. The numerical model validation was performed on the experimental data of Pelfrey and Liburdy (1986) for a single offset jet (SOJ). The main purpose of Kumar (2015) study was to picked out the wall jet addition influence on the whole combined wall and offset jets flow (WOJ) characteristics. It has been proved that the wall jet addition result in a deviation of the offset jet toward the horizontal wall with higher intensity which decreases for elevated offset ratio values. Numerical correlations for the merge point, the combined points and the recirculation vortices positions was also performed with respect to the offset ratio H.

Mondal *et al.* (2015) numerically studied the velocity ratio effect on the mutual interaction between the wall jet and the offset jet in 2D WOJ flow with the unsteady RANS method. The non-dimensional nozzle spacing and the Reynolds number are respectively set to 1 and 10000. The velocity ratio was varied by modifying the wall jet exit velocity while keeping fix that of the offset jet. This parameter presents the ratio between the wall jet exit velocity and that of the offset jet. The numerical results provided by Mondal *et al.*

(2015) showed that for velocity ratio ranged between 0.78 and 1.34, Karman vortex shedding are noted along the converging zone. On the other hand, for velocity ratio values less than 0.77 and greater than 1.35, this phenomenon disappeared while for velocity ratio equal to 0.77 or 0.35, two stable and counter rotated vortices was formed along the converging flow zone.

Mondal *et al*. (2016) have numerically simulated turbulent multi-jets flow which combine a wall and an offset jets flow (WOJ). Their numerical model was validation on the experimental setup of Wang and Tan (2007) and the numerical data of Li *et al*. (2011). The considered Reynolds number was taken equal to 10000, the offset jet nozzle width is set to 1 and the wall jet nozzle width is varied between 0.2 and 2. The authors have noted a decreases in the merge point longitudinal location when increases the wall jet width. Moreover, for wall jet nozzle non-dimensional width equal to 0.2, the WOJ flow remains steady and two stable counter rotating vortices appear along the converging zone. On the other hand, for wall jet nozzle width between 0.3 and 1, an unsteady large scale von Karman-like vortex shedding phenomenon is observed along the same zone.

Through all the above mentioned works, it appears that the majority of the studies on combined wall and offset jets flow (WOJ) have only focused on the influence of the jets spacing as well as the velocity ratio on the different characteristics of this flow. Based on above literature survey and author's knowledge, there are no significant attempt to study the wall inclination effect on WOJ flow characteristics. Thus, the main purpose of the present investigation is to fill these gaps by studying the wall inclination effect on the WOJ maximum velocity decay and the different shear layers spreading. A major interest is also given to the comparison between a single offset jet flow (SOJ) and combined wall and offset jets flow (WOJ).

2. MATHEMATICAL FORMULATION

The geometric configuration (Fig. 1) of combined wall and offset jet flow (WOJ) realized by Kumar (2015) is used to numerically study the influence of the wall inclination β on the dynamic characteristics of the WOJ flow. The wall jet (denoted LWJ: Lower Wall Jet) and the offset jet (denoted UOJ: Upper Offset Jet) are ejected from twin identical and rectangular nozzles (Fig. 1). The width and length of each nozzle was respectively d=12.5mm and l=150mm. Both nozzles are contained in the transverse plane (x=0). The offset ratio is set to h=9×d. We note that the previously mentioned parameter is defined as the distance between the horizontal wall (at y=0) and the lower extremity of the offset jet (UOJ).

The domain dimensions along the longitudinal and the transverse direction are carefully chosen by avoiding to affect the WOJ flow spreading. Several dimensions were tested before finally adopting 100×d and 50×d respectively along the longitudinal and the transverse directions (Fig. 1). The equations system managing the present investigated flow is written with respect the Cartesian coordinate system whose origin o is located on the wall axis (Fig. 2). During the present investigation, the following assumptions are adopted

(1) The flow is supposed two dimensional (2D) and steady.

(2) The work fluid is air (Pr=0.7) with constant density (incompressible flow).

(3) The flow is assumed fully developed and in turbulent regime.

By considering the above cited conditions, the governing equations in Cartesian tensor form can be written as follow:

$$\frac{\partial}{\partial x_i}\left(\rho u_i\right)=0 \tag{1}$$

$$\frac{\partial}{\partial x_j}\left(\rho u_i u_j\right)=-\frac{\partial p}{\partial x_i}+\frac{\partial}{\partial x_j}\left[\mu\left(\frac{\partial u_i}{\partial x_j}+\frac{\partial u_j}{\partial x_i}-\frac{2}{3}\delta_{ij}\frac{\partial u_l}{\partial x_l}\right)\right]+\frac{\partial}{\partial x_j}\left(-\rho\overline{u_i' u_j'}\right) \tag{2}$$

Boussinesq approximation is used to link the Reynolds stress (Eq. (2)) to the mean velocity gradient as follow:

$$-\overline{\rho u_i' u_j'}=\mu_t\left(\frac{\partial u_i}{\partial x_j}+\frac{\partial u_j}{\partial x_i}\right)-\frac{2}{3}\left(\rho k+\mu_t\frac{\partial u_k}{\partial x_k}\right)\delta_{ij} \tag{3}$$

The turbulent kinetic energy k and its specific dissipation rate ω are picket out respectively from the following transport equations:

$$\frac{\partial}{\partial x_i}\left(\rho k u_i\right)=\frac{\partial}{\partial x_j}\left(\Gamma_k\frac{\partial k}{\partial x_j}\right)+G_k-Y_k+S_k \tag{4}$$

$$\frac{\partial}{\partial x_i}\left(\rho \omega u_i\right)=\frac{\partial}{\partial x_j}\left(\Gamma_\omega\frac{\partial \omega}{\partial x_j}\right)+G_\omega-Y_\omega+S_\omega \tag{5}$$

G_k and G_ω respectively in Eqs. (4) and (5) are the generation of the turbulent kinetic energy k and its specific dissipation rate ω k owing to the mean velocity gradient.

On the other hand, Γ_k and Γ_ω are the effective diffusivity for k and ω. In addition, Y_k and Y_ω are respectively the k and ω dissipation owing to the turbulence. Remain to define S_k and S_ω which

$$\Gamma_k=\mu+\frac{\mu_t}{\sigma_k} \tag{6}$$

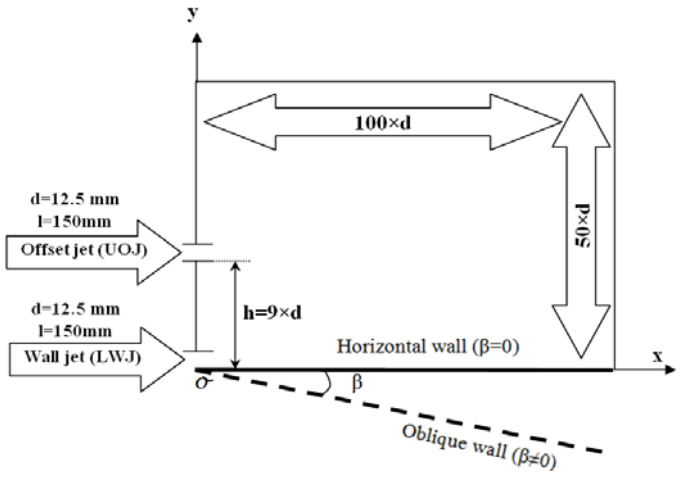

Fig. 1. Geometric configuration used for numerical model validation

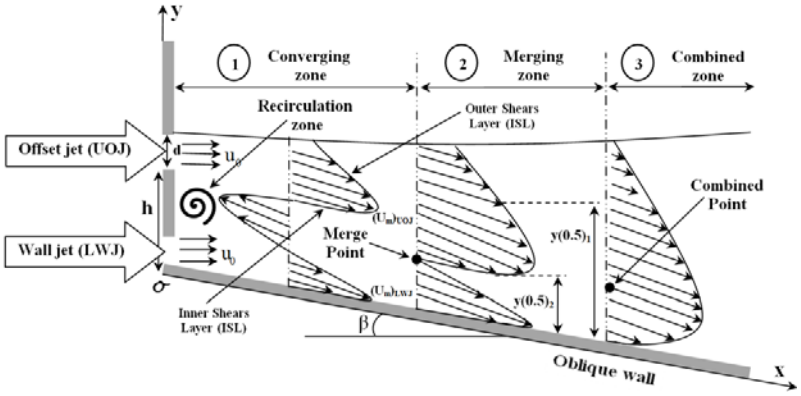

Fig. 2. Combined wall and offset jet (WOJ) flow diagram

$$\Gamma_\omega = \mu + \frac{\mu_t}{\sigma_\omega} \tag{7}$$

$$\mu_t = \alpha^* \frac{\rho k}{\omega} \tag{8}$$

present the source terms. The effective diffusivity as well as the turbulent viscosity are defined as follow: The constant values $\sigma_k=\sigma_\omega=2$ are the turbulent Prandtl numbers respectively for k and ω. Moreover, α^* is given by the following expression:

$$\alpha^* = \alpha_\infty^* \left(\frac{\alpha^*_0 + \mathrm{Re_t}/\mathrm{R_k}}{1 + \mathrm{Re_t}/\mathrm{R_k}} \right) \tag{9}$$

$$\mathrm{Re_t} = \frac{\rho k}{\mu \omega} \tag{10}$$

$$\alpha^*_0 = \frac{\beta_i}{3} \tag{11}$$

The constant values are defined as $R_k=6$ and $\beta_i=0.072$. In the case of high Reynolds number k-ω turbulence model we consider that $\alpha^* = \alpha_\infty^* = 1$. In Eqs. (4-5), G_k and G_ω are defined by the following expression:

$$G_k = -\rho \overline{u_i' u_j'} \frac{\partial u_j}{\partial x_i} \tag{12}$$

$$G_k = \mu_t S^2 \tag{13}$$

$$S \equiv \sqrt{2 S_{ij} S_{ij}} \tag{14}$$

$$G_\omega = \alpha \frac{\omega}{k} G_k \tag{15}$$

$$\alpha = \frac{\alpha_\infty}{\alpha^*} \left(\frac{\alpha_0 + \mathrm{Re_t}/\mathrm{R_\omega}}{1 + \mathrm{Re_t}/\mathrm{R_\omega}} \right) \tag{16}$$

Note that $R_\omega=2.95$, $\alpha_\infty = 0.52$ and $\alpha_0=1/9$ are constant values and α^* as well as $\mathrm{Re_t}$ are respectively provided by Eqs. (9) and (10). It seems also important to note that $\alpha=\alpha^*=1$ for high Reynolds number k-ω turbulence model. The k-ω model details are given in FLUENT 6.3.26 user's guide.

As detailed in Fig. 3, a non-uniform mesh is applied along the x (longitudinal direction) and y (transverse direction) axis. Small grid size is adopted on the nozzle plate vicinity and higher one is applied further downstream. Constant grid spacing (a=0.05) is applied on [A], [B] and [C] segments while non-uniform one is considered on [D] segment with a grid spacing a=0.5 and an expansion ratio e=1.045. The [E] segment has also non-uniform mesh with a grid spacing and expansion ratio respectively equal to a=0.5 and

e=1.0185. It seems important to note that opposite segments are identical in term of grid spacing (Fig. 3). The whole domain cell number is given by the as following equation:

$$N_{totale} = (N_A + N_B + N_C + N_D) \times N_E = 280 \times 200 = 56000 \quad (17)$$

Note that this particular choice of nodes number is not random and it will be discussed later along the grid size sensitivity test section. To complete the simulated model, besides the equations mentioned above, it remains only to take into account the boundary conditions which are minutely detailed in Fig. 3 and Table 1.

The transport equations, associated to the boundaries and emission conditions are numerically resolved based on the finite volume method developed by Pantakar (1980) using the CFD software FLUENT 6.3.26. The numerical domain is divided into a finite number of sub-zones called "the control volume". The principle of the resolution method is to integrate, on each control volume, the transport equations such as those of the momentum conservation, the mass conservation, the turbulent kinetic energy k and its specific dissipation rate ω. The mentioned equations are discretized with the help of the second order UPWIND. Moreover, the velocity-pressure coupling is based on the SIMPLEC algorithm and the global solution convergence is reached when the normalized residuals fall below 10^{-4}.

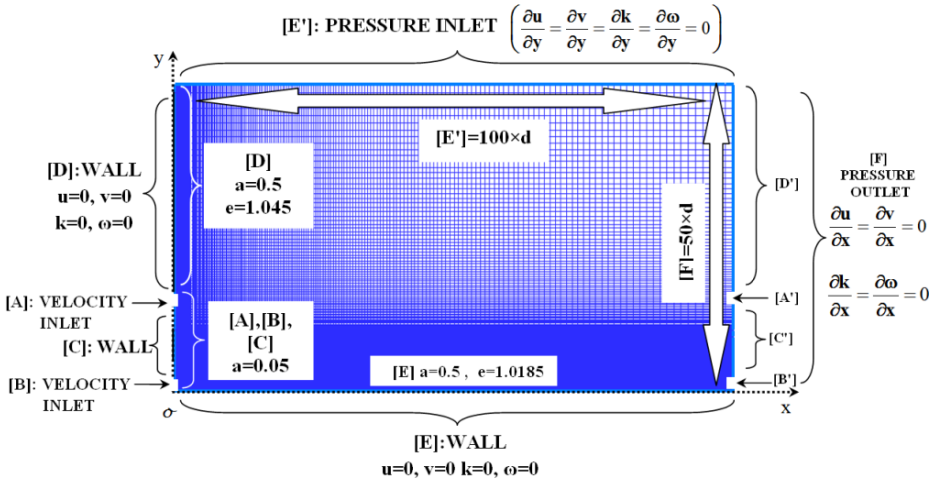

Fig. 3. Grid size and boundary conditions details

Table 1 Boundary and emission conditions.

Boundary conditions			Details
[A] and [B]	Nozzles outlet	**VELOCITY INLET**	$u_0 = 17.4\,m/s$
			$k_0 = \frac{3}{2}(IU_0)^2 = 1.135\,m^2/s^2$
			$\omega_0 = \frac{k_0^{1/2}}{C_\mu^{1/4} l} = 1203.1\,\frac{1}{s}$
[C] and [D]	Nozzles plate	**WALL**	u = 0 , v = 0 , k = 0 , ω = 0
[E]	Oblique wall	**WALL**	u = 0 , v = 0 , k = 0 , ω = 0
[E']	Lateral face (y=50×d)	**PRESSURE INLET**	$P = P_{amb}$ $\frac{\partial u}{\partial y}=\frac{\partial v}{\partial y}=\frac{\partial k}{\partial y}=\frac{\partial \omega}{\partial y}=0$
[F]	Flow outlet (x=100×d)	**PRESSURE OUTLET**	$P = P_{amb}$ $\frac{\partial u}{\partial x}=\frac{\partial v}{\partial x}=\frac{\partial k}{\partial x}=\frac{\partial \omega}{\partial x}=0$

3. RESULTS AND DISCUSSIONS

3.1. Velocity Field Validation and Grid Sensitivity Test

We show in Fig. 4a the transverse evolution of the non-dimensional longitudinal velocity U along the plane X=7 for an offset ratio and a Reynolds number respectively equal to H=9 and Re=15000. Using the standard k-ω turbulence model, the velocity profile is plotted with (180×125), (280×200) and (330×333) grid sizes. These mentioned grids respectively contain 22 500, 56 000 and 109 800 quadratic cells. It seems clear from Fig. 4a that the velocity profile obtained by (280×200) and (330×333) grid sizes

are almost identical while a notable discrepancy was detected between (180×125) and (280×200). The maximum error detected between the results of Kumar (2015) and those given in the present study by (180×125) grid size is 7.3% while it is smaller than 1.3% for the other grid (280×200 and 330×333). Consequently, we can say that the grid convergence is reached at the (280×200) grid size.

The same longitudinal velocity profile validation is showed in Fig. 4b with the selected grid size (280×200) and using several turbulence models such as the standard k-ω, the SST k-ω, the standard k-ε, the RNG k-ε and the realizable k-ε. It is clear from this figure that, except the k-ε realizable witch over-predicts the velocity profile, the longitudinal velocity predicted by the presented turbulence models are in agreement with Kumar (2015) results for 2.5≤Y≤5. Whereas beyond Y=5, the standard k-ω model provides the best concordance with Kumar (2015) results. Thus, the standard k-ω turbulence model associated to the selected grid size (280×200) will be adopted in all calculation.

3.2. Mean Flow Structure

Combined wall and offset jets (WOJ) flow is formed by three relevant zones (Wang and Tan (2007), Vishnuvardhanarao and Das (2009), Kumar and Das (2011), Mondal and Das (2014), Kumar (2015) and Zhiwei (2011)) (Fig. 1). The initial flow region is called the converging zone wherein the wall jet and the offset jet are attracted towards each other. This initial flow region is characterized by reverse flow and lower pressure due to the training of the fluid existing between the wall jet and the offset jet. At the end of this zone we found the merge point (denoted MP) at which the inner shear layers of the wall jet and the offset jet meet. Beyond the MP, a second flow zone called the merging zone appears. Along this region, the two jets merging process takes place and ends at a second point called the combined point (denoted CP). Beyond the combined point, the latter flow zone (the combined zone) started. Along this region, the whole WOJ flow behaves as a single wall jet.

3.2. Wall Inclination Effect on Maximum Velocity Decay

3.2.1. Comparison With Previous Investigations

Comparison between the present numerical results concerning the maximum velocity U_m for single offset jet (SOJ) flow and the experimental results of Pelfery and Liburdy (1986), Nasr and Lai (1997) in addition to the numerical ones performed by Pramanik and Das (2013) is shown in Fig. 5a. It is clear from this figure that the present maximum velocity U_m prediction for horizontal wall (β=0) present good agreement with Pelfery and Liburdy (1986) results beyond à longitudinal position X=3 while it over-predicts the results of Nasr and Lai (1997). For wall inclination β=10, a satisfactory agreement is also observed for $3 \leq X \leq 8$ between our results and those of Pramanik and Das (2013) while some discrepancy is noticed outside this interval.

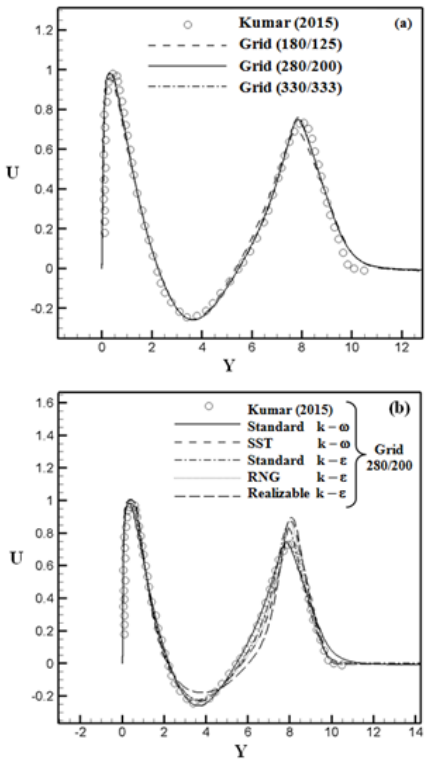

Fig. 4. Longitudinal velocity validation (a) Grid size sensitivity (b) Turbulence model sensitivity.

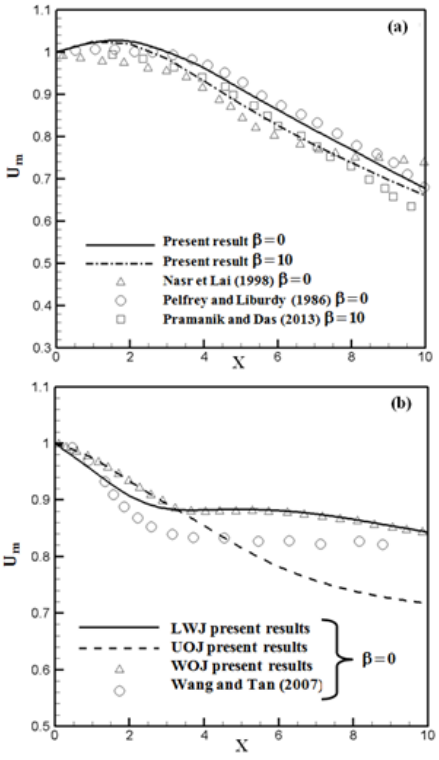

Fig. 5. Maximum velocity decay for single offset jet flow SOJ (a) and combined wall and offset jet flow WOJ (b)

Figure 5b shows our numerical results concerning the maximum velocity decay for WOJ flow alongside the experimental results proposed by

Wang and Tan (2007) for zero wall inclination. According to authors' knowledge, except the present work, there are no experimental or numerical studies that investigate the WOJ flow for different wall inclinations. Our prediction (Fig. 5b) shows that for X≤3, the WOJ flow maximum velocity is decided by the offset jet UOJ (because the UOJ present the higher U_m value), whereas beyond X=3, the maximum velocity will be decided by the wall jet LWJ (because the LWJ becomes the one with the higher U_m value). It is then possible to reconstruct the U_m curve for the whole WOJ flow as shown in Fig. 5b.

Despite the presence of the constant U_m values that is already noticed by Wang and Tan (2007) and which has amplitude U_m=0.8 (in the present work U_m = 0.88), a discrepancy between our results and those of Wang and Tan (2007) is noticed. This difference may be related to the inaccuracy of the experimental measurement techniques used in the recirculation zone characterized by high turbulence level. Wang and Tan (2007) used PIV technique with an uncertainty of 5% and 10% respectively for the average velocity and the turbulent quantities measures.

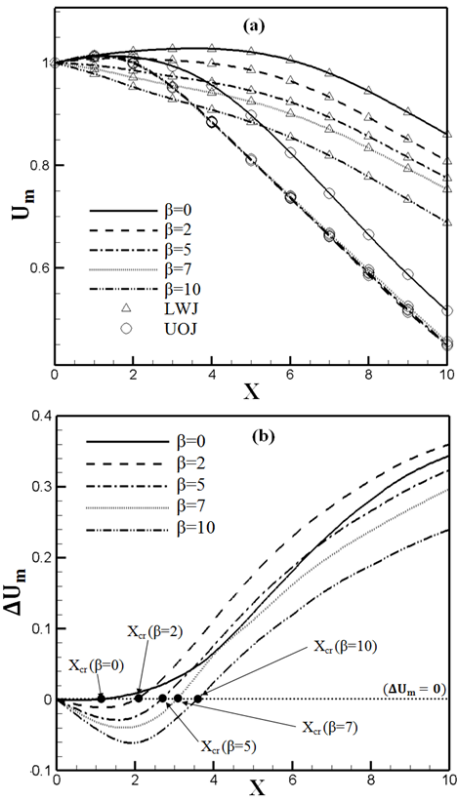

Fig. 6. Wall inclination effect on maximum velocity decay (a) and maximum velocity difference between the UOJ and the LWJ (b)

The longitudinal distribution of the maximum velocity U_m of the offset jet (UOJ) and that of the wall jet (LWJ) along the converging zone of the WOJ flow is shown in Fig. 6a for different wall inclinations β. This figure shows that U_m continuously decreases as the flow expands along the longitudinal direction (X increases), in addition the maximum velocity decreases faster when increasing the wall inclination β. This is in good agreement with Nasr and Lai (2000) study for single offset jet (SOJ) flow. These authors noticed acceleration in the maximum velocity decay for higher wall inclination β values.

It is obvious that the maximum velocity of the WOJ flow is influenced by the jet (UOJ or LWJ) which has the higher U_m value. As shown in Fig. 6a, just in the nozzle plate vicinity zone, there is a kind of "competition" between the amplitudes of the UOJ and LWJ maximum velocities. In order to highlight this phenomenon, we represent in Fig. 6b along the same flow zone, the longitudinal variation of the difference between the UOJ and the LWJ maximum velocity ($\Delta U=(U_m)_{LWJ} - (U_m)_{UOJ}$). It is clear from Fig. 6b that for all considered wall inclinations β and beyond certain critical longitudinal position denoted X_{cr}, the flow maximum velocity is decided by the wall jet LWJ ($\Delta U_m>0$). The critical position X_{cr} varies as a function of β following a polynomial function:

$$X_{cr} = -0.01\beta^2 + 0.324\beta + 1.346 \quad (18)$$

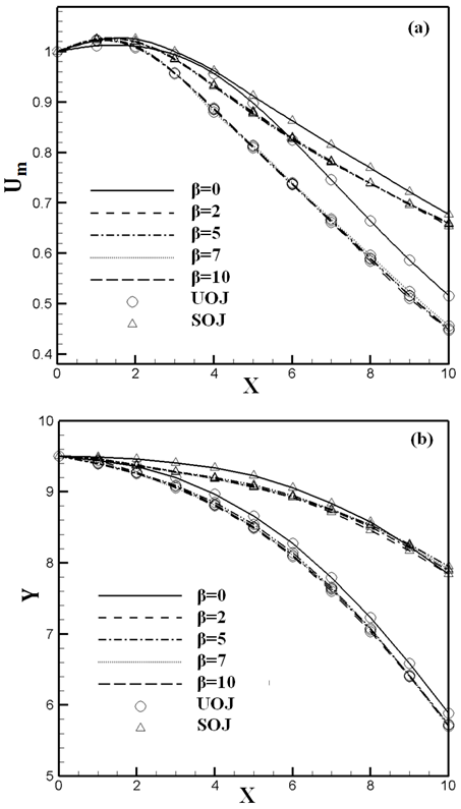

Fig. 7. Maximum velocity decay (a) and maximum velocity trajectory (b) for single offset jet SOJ and combined wall and offset jet WOJ.

On the other hand, for X<X_{cr}, the maximum velocity of the WOJ flow is decided by the offset jet UOJ (ΔU_m<0) (Fig. 6b). It is also important to note that the maximum velocity of the LWJ and that of the UOJ experience a certain increase which exceeds the value U_m=1 at the nozzles ejection and reaches maximum value whose amplitude and longitudinal position decreases when increasing the wall inclination. This was also noted by Kumar

(2015) for WOJ flow with horizontal wall (β=0). This author found that this maximum velocity value decreases in amplitude and longitudinal position for higher offset ratio H value.

3.2.2. Comparison Between Single Offset Jet (SOJ) and Combined Wall and Offset Jets (WOJ) Flows

In order to make a comparison between the offset jet behaviors when this latter (UOJ) is combined to a wall jet (LWJ) (to form a WOJ flow) and when the LWJ is absent (SOJ flow), Fig. 7 shows the longitudinal evolution of the offset jet maximum velocity U_m (Fig. 7a) and its trajectory $\left(X_{U_m}, Y_{U_m}\right)$ (Fig. 7b) in WOJ and SOJ flows cases. It can be seen from Fig. 7a that, for all considered wall inclinations β, the offset jet maximum velocity for SOJ flow is greater than that for WOJ flow, while in the case of WOJ, the maximum velocity U_m decreases faster than that for SOJ flow. The trajectory followed by the offset jet maximum velocity U_m shown in Fig. 7b reported a stronger deviation (Y_{U_m} cure slope is higher) of the offset jet in WOJ flow case compared to that of SOJ. This can be explained from the static pressure contours shown in Fig. 8, this figure shows that the wall jet (LWJ) addition next to the offset jet (UOJ) (change from SOJ to WOJ flow) makes the recirculation zone more sub-atmospheric (higher depression). As shown in Fig. 8, for β=0, the minimum pressure along the recirculation zone is equal to P_{min}=-80×10^{-3} (Fig. 8a) in the case of WOJ flow and P_{min}=-69.1×10^{-3} (Fig. 8c) in the SOJ flow case. This difference in the depression results that the deviation of the offset jet in the case of WOJ flow is more intense than that in SOJ flow. This leads us to conclude that the effect of the wall jet (LWJ) on the offset jet (UOJ) in a WOJ flow is greater than the effect of the oblique wall (called the Coanda Effect) in SOJ flow.

3.3. Wall inclination effect on the flow spreading

3.3.1. Comparison Between Single Offset Jet (SOJ) and Combined Wall and Offset Jets (WOJ) Flows

Throughout the following section the outer and inner shear layers on the offset jet (UOJ) side in WOJ flow will be respectively denoted ISL (Inner Shear Layer) and OSL (Outer Shear Layer). As shown in Fig. 1, two dynamic half-widths are identified $Y(0.5)_1$ and $Y(0.5)_2$ respectively for the OSL and the ISL of the offset jet (UOJ).

The longitudinal distribution of the dynamic half-widths $Y(0.5)_1$ (Fig. 9a) and $Y(0.5)_2$ (Fig. 9b) along the convergence zone in WOJ and SOJ shows that increasing the wall inclination is accompanied by an increase in $Y(0.5)_1$ and $Y(0.5)_2$. This means that elevating the wall inclination β results in a weakening of the outer shear layers (OSL) and the inner shear layers (ISL) deflection and consequently a better propagation of these shear layers in both single offset jet (SOJ) and combined wall and offset jet (WOJ) flows cases. This effect of the wall inclination on the deflection of the OSL and ISL can be explained base on the static pressure contours in Fig. 8. From this figure, it can be seen that in both SOJ and WOJ flow cases, when the wall inclination β increases, the recirculation zone depression is lower. For WOJ flow, the minimum pressure is equal to P_{min}=-80×10^{-3} (Fig. 8a) and P_{min}=-74.3×10^{-3} (Fig. 8b) respectively for β=0 and β=7. For single offset jet (SOJ) flow, this minimum pressure change from P_{min}=-69.1×10^{-3} (Fig. 8c) for β=0 to P_{min}=-57.9×10^{-3} for β=10 (Fig. 8d). Consequently the OSL and ISL for higher wall inclinations β values are less deviated and consequently more spread. It is also clear from Fig. 9 that for constant wall inclination β, the half widths $Y(0.5)_1$ and $Y(0.5)_2$ in SOJ flow are always higher than those in WOJ. That means a lower deflection and consequently a better spread of the OSL and ISL in a SOJ flow compared to WOJ flow.

3.3.2. Comparison Between the Outer Shear Layers (OSL) and the Inner Shear Layers (ISL) Spreading

Figure 10 presents, the longitudinal evolution of the dynamic half-widths $Y(0.5)_1$ and $Y(0.5)_2$ along the convergence zone in the case of SOJ (Fig 10a) and WOJ (Fig. 10b) flows. It can be seen from this figure that $Y(0.5)_1$ remains always higher that $Y(0.5)_2$ for both WOJ and SOJ flows, which mean that the outer shear layers (OSL) spreading is better than that of the inner shear layers (ISL). This spreading difference between the outer (OSL) and the inner (ISL) was also noted by Swayer (1960) and Nasr and Lai (1998) in single offset jet (SOJ) flow. These authors observed a better spreading of the offset jet in the convex side (OSL) compared to the concave side (ISL). Furthermore, Pelfery and Liburdy (1986) find higher values of Reynolds stress $\overline{u'u'}$, $\overline{v'v'}$ and $\overline{u'v'}$ at the OSL compared to the ISL in SOJ flow case. According to Pelfery and Liburdy (1986), this is due to the asymmetric influence of the streamlines deviation at the ISL (stabilizing effect) and the OSL (destabilizing effect). On the other hand, Pramanik and Das (2013) noted higher turbulence level at the OSL (11.5%) compared to the ISL (4.5%), which means a better entrainment rate of the surrounding fluid at the outer shear layers (OSL) compared to the inner shear layers (ISL), therefore a better OSL spreading compared to the ISL.

4. CONCLUSION

A CFD simulation of a turbulent 2D WOJ flow combining an offset jet (UOJ) and an oblique wall jet (LWJ) has been performed. The main objective of this numerical study is to investigate the wall inclination β effect on the maximum velocity decay as well as the inner and outer shear layers spreading. Some important results had been obtained as follow:

- Beyond a critical longitudinal position X_{cr}, the WOJ flow maximum velocity is decided by the wall jet (LWJ). The longitudinal position X_{cr} varies as a function of the wall inclination following polynomial function described by Eq. (18). While for $X<X_{cr}$, the maximum velocity of the WOJ flow

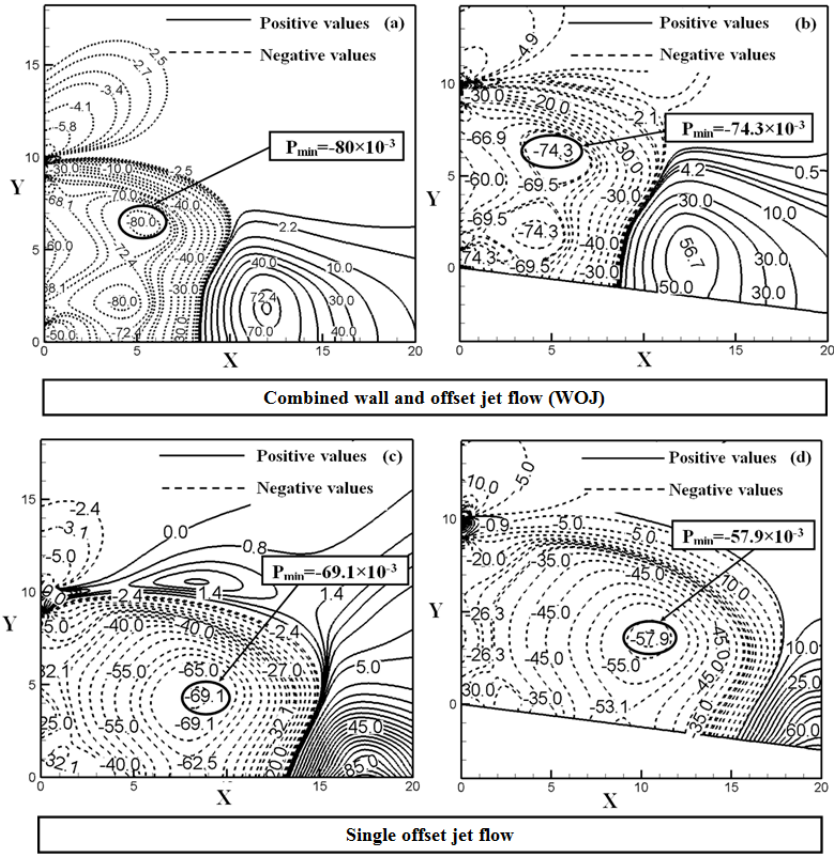

Fig. 8. Static pressure contours (1000×P) along the converging zone (a, c) Horizontal wall β=0 (b, d) Oblique wall β=7

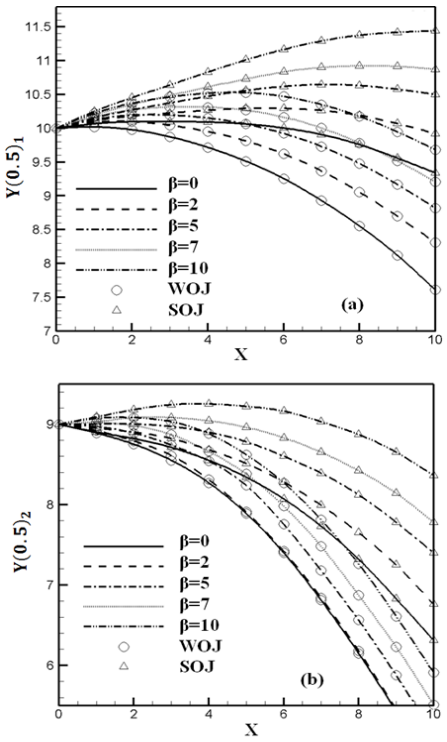

Fig. 9. Wall inclination effect on the outer $Y(0.5)_1$ (a) and inner $Y(0.5)_2$ (b) shear layers spreading for both single offset jet SOJ and combined wall and offset jet flows

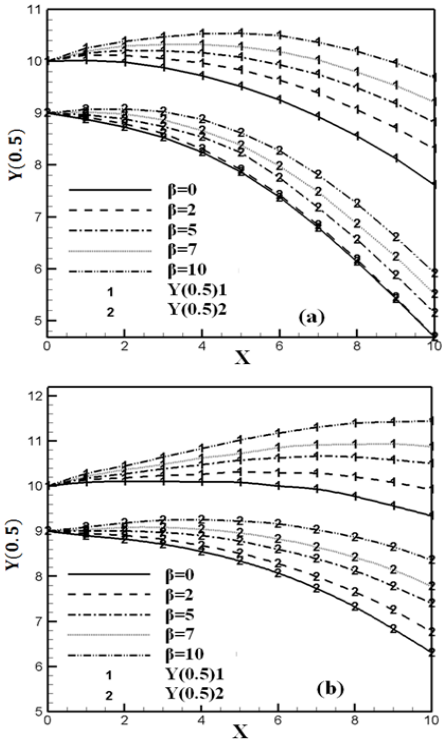

Fig. 10. Wall inclination effect on the outer $Y(0.5)_1$ and inner $Y(0.5)_2$ shear layer spreading for single offset jet SOJ (a) and combined wall and offset jet (b) flows

is decided by the offset jet (UOJ).

- The maximum velocity of the LWJ and that of the UOJ experiences a certain increase which exceeds the value U_m=1 at the nozzles ejection and reaches maximum value whose amplitude and longitudinal position decrease when increasing the wall inclination β.

- Along the converging zone and for all considered wall inclinations β, the offset jet maximum velocity for SOJ flow is greater than that in WOJ flow, while for WOJ flow, the maximum velocity U_m decreases faster than that for SOJ flow. Furthermore, a lower deflection and consequently a better spreading of the OSL and ISL in single offset jet (SOJ) flow compared to combined wall and offset jet (WOJ) flow.

- For both WOJ and SOJ flows, elevating the wall inclination β results in a weakening of the outer shear layers (OSL) and the inner shear layers (ISL) deflection and consequently a better spreading of these shear layers. On the other hand, the outer shear layers (OSL) spreading is better than that of the inner shear layers (ISL).

REFERENCES

Kumar A. (2015), Mean flow characteristics of a turbulent dual jet consisting of a plane wall jet and a parallel offset jet. *Computers and fluids*. 114. 48–65.

Kumar A. and M. K. Das (2011), Study of a turbulent dual jet consisting of a wall jet and an offset jet*. Journal Fluids Eng. 133*.1201-1211.

Mondal T. and M. K. Das (2014), Numerical Investigation of Steady and Periodically Unsteady flow for various separation distances between a wall and an offset jet. *Journal of fluid and structure* 50. 528-546.

Modal T., A. Guha and Das (2015), Computational Study of periodically unsteady interaction between a wall jet and offset jet for various velocity ratio. *Computers and fluids* 123.146-161.

Modal T., A. Guha, M. K. Das (2016), Effect of bottom wall proximity ion the unsteady flow structure of a combined turbulent wall jet and offset jet flow. *European journal of Mechanics B/Fluids* 57. 101-114.

Nasr, A. and J. C. S. Lai (1997), Comparison of flow field characteristics in the near field of two parallel plane jets and an offset plane jet. *Physics of Fluids* 9. 2219-2231.

Nasr, A., J. C. S. Lai (2000), The effects of wall inclination on an inclined offset jet. In: 10th *International symposium on application of laser techniques to fluid mechanics*.

Nasr, A., J. C. Lai S. A. (1998), Turbulent plane offset jet with small offset ratio. *Experiments in Fluids. 24*. 47-57.

Patankar, S. (1980), *Numerical Heat Transfer and Fluid Flow*, Hemisphere, New York.

Pelfrey, J. R. R. and J. A. Liburdy (1986), Effect of curvature on the turbulence of a two-dimensional jet, *Journal of Fluid Engineering. 3*. 143–9.

Pramanik, S. and M. K. Das (2013), Numerical characterization of a planar turbulent offset jet over an oblique wall. *Computer and Fluids* 77. 36–55.

Sawyer, R. A. (1960), The flow due to a two-dimensional jets issuing parallel to a flat plate. *Journal Fluid Mechanics 9*. 543-561.

Vishnuvardhanarao, E. and M. K. Das (2008), Computation of Mean Flow and Thermal Characteristics of Incompressible Turbulent Offset Jet Flows. *Numerical Heat Transfer: Part A.* 53. 843–869.

Vishnuvardhanarao, E. and M. K. Das (2009), Study of the heat transfer characteristics in turbulent combined wall and offset jet flows. *International Journal of Thermal Sciences*. 48. 1949–1959.

Wang, X. and S. Tan (2007), Experimental Investigation of the Interaction Between a Plane Wall Jet and a Parallel Offset Jet. *Experiments in Fluids. 4*. 551–562.

Zhiwei, L., W. Huai, J. Han (2011), Large eddy simulation of the interaction between wall jet and offset jet. *Journal of hydrodynamics. 23*. 544-553.